Inverse Perspective Mapping Roll Angle Estimation for Motorcycles

Citation	Damon, Pierre-Marie, Hadj-Abdelkader, Hicham, Arioui, Hichem and Youcef-Toumi, Kamal. 2018. "Inverse Perspective Mapping Roll Angle Estimation for Motorcycles." 2018 15th International Conference on Control, Automation, Robotics and Vision, ICARCV 2018.
As Published	10.1109/icarcv.2018.8581182
Publisher	Institute of Electrical and Electronics Engineers (IEEE)
Version	Author's final manuscript
Citable link	https://hdl.handle.net/1721.1/137988
Terms of Use	Creative Commons Attribution-Noncommercial-Share Alike
Detailed Terms	http://creativecommons.org/licenses/by-nc-sa/4.0/

Inverse Perspective Mapping Roll Angle Estimation for Motorcycles

Pierre-Marie Damon[1,2], Hicham Hadj-Abdelkader[1], Hichem Arioui[1] and Kamal Youcef-Toumi[2]

Abstract— This paper presents an image-based approach to estimate the motorcycle roll angle. The algorithm estimates directly the absolute roll to the road plane by means of a basic monocular camera. This means that the estimated roll angle is not affected by the road bank which is often a problem for vehicle observation and control purposes. For each captured image, the algorithm uses a numeric roll loop based on some simple knowledge of the road geometry. For each iteration, a bird-eye-view of the road is generated with the inverse perspective mapping technique. Then, a road marker filter associated with the well-known clothoid model are used respectively to track the road separation lanes and approximate them with mathematical functions. Finally, the algorithm computes two distinct areas between the two-road separation lanes. Its performances are tested by means of the motorcycle simulator BikeSim. This approach is very promising since it does not require any vehicle or tire model and is free of restrictive assumptions on the dynamics.

I. INTRODUCTION

Road accidents have always been a major concern all around the world. To overcome this issue automotive engineers never ceased to innovate about vehicle safety while improving driving experience and comfort. In this context, car makers began to equip P4WV with the well-known Advanced Driver Assistance Systems (ADAS). Among the most popular ADAS, we can cite: the Anti-lock Braking System (ABS), the Electronic Stability Program (ESP) or the Electronic Stability Control (ESC), etc.

Nevertheless, Powered Two-Wheeled Vehicles (P2WV) industry did not follow the same trend. Nowadays, the lack of Advanced Rider Assistance Systems (ARAS) makes the P2WV the most deadly means of transportation. Several arguments can explain the difficulties that motorcycle makers have in developing ARAS. First of all, the technical and economical reasons, P2WV are supposed to be cheaper and more compact than other motor vehicle. Moreover, motorcycle motion is very complex because of the lateral dynamics making the P2WV modeling highly complicated. The second reason is the rider acceptance [1]. Indeed, few ARAS already exist on the market but their success is very contested. Hence, the big challenge for P2WV researchers is to develop new ARAS that assist the riders during critical situations without interfering with their feelings.

This paper is organized as follows. Section 2 presents the motivations and defines the problem. The inverse perspective mapping technique, the road marker filtering and the fitting step are addressed in section 3. Whereas in section 4, we will discuss the algorithm performing the roll angle

estimation. Then in section 5, simulations carried out with the advanced motorcycle simulator "BikeSim" are discussed. Finally, concluding remarks are summarized in section 6.

II. MOTIVATION AND PROBLEM STATEMENT

In the context of ARAS development, the observers and estimators turn out to be essential tools. Indeed, they allow to replace some costly sensors or even estimate unmeasurable dynamics like the tire's forces. When investigating the lateral P2WV dynamics, it appears that one of the most important risk indicator is the roll angle. That is why, for the research community, the first big challenge was to address the estimation of the P2WV lean angle.

In 2008, precursor work was published about this topic in [2]. Then, in a chronological order, it was investigated in [3], [4], [5] and more recently in [6], [7], [8], [9]. In all of these works, authors proposed various observation techniques but all of them used a model-based design. Note that, in addition to several restrictive assumptions on the dynamics, they require a complex process to identify the model parameters.

In [10], the author was the only one to propose an alternative to this model-based design by introducing a video-based roll angle estimator for the P2WV. The technique requires a learning step to correlate the orientation statistics in the image and the actual roll angle. Then, the roll estimation is deduced from gradient orientation histograms by correlating the current image with the learned data. Then, in [11], the same author proposed to compare his video-based results with the Inertial Measurement Unit (IMU) measures. On the same topic, some works have addressed P4WV orientation estimation. We can cite [12], where the author introduced an algorithm to simultaneously estimate the vehicle roll, yaw and pitch angles with a monocular camera. Nevertheless, this technique works for a small roll range and consequently, cannot be used for motorcycle estimation purposes.

Most of the proposed solutions cited above require a multi-sensor instrumentation to perform the roll angle estimation. They require a steering encoder, a speedometer, a gyroscope, etc. which make these solutions still expensive and more prone to mechanical failures. In addition, they are model-based which means the observers are synthesized using a model of the P2WV. This design involves advanced robustness studies taking into account the modeling assumptions (linear approximations, etc.) and the uncertainties (rider weight, inertia, etc.). Most of the time, the results have shown that the performances remind acceptable in a small range around the nominal case used for the design. As cited above, in [10], [11], the author has proposed a vision-based

approach that does not use a P2WV model or, even, any heavy instrumentation. Nevertheless, the proposed approach is fairly binding because it requires a learning step and the performances are degraded in the case where the current situation does not directly correspond to one ever learned.

This paper introduces a new original solution to estimate the P2WV roll angle by means of a simple monocular camera without the use of any other sensors. It is capable of estimating the absolute roll angle without any information about the previous sample or the initial condition. The algorithm computes an approximate Bird-Eye-View (BEV) of the road by means of the Inverse Perspective Mapping (IPM) technique. Then, it uses the knowledge of road geometry to recover the absolute roll between the vehicle and the road. Unlike the solution proposed in [10], [11], the algorithm does not require any initialization step or any data base.

III. INVERSE PERSPECTIVE MAPPING AND LANE DETECTION AND FITTING

A. Inverse perspective mapping

Let us consider a conventional camera attached to the frame $\mathcal{F}_c$. Its intrinsic parameters are given by the calibration matrix $\mathbf{K}$, whereas its extrinsic ones are given by the rotation matrix $\mathbf{R} \in \mathbb{SO}(3)$ and the translation vector $\mathbf{t} \in \mathbb{R}^3$ with respect to the world frame $\mathcal{F}_w$. For the sake of simplicity, the camera distortions are not considered in this study. Nevertheless, one can note that distortion parameters can be obtained after camera calibration. Let P be a 3D point of coordinates $\mathbf{P} = (X\ Y\ Z)^\top$ in the world frame $\mathcal{F}_w$. The image formation of the 3D point P is obtained through its projection into the 2D point p of homogeneous coordinates $\mathbf{p} = (u\ v\ 1)^\top$ in the image plane $\mathcal{F}_i$. The projection equation is given by:

$$\mathbf{p} \propto \mathbf{K}\,(\mathbf{R}\,\mathbf{P} + \mathbf{t}) \tag{1}$$

where $\propto$ denotes the equality up to scale and $\mathbf{K}$ is the camera calibration matrix. Its expression is given in [13].

The IPM warps p into a new point p' of homogeneous coordinates $\mathbf{p}' = (u'\ v'\ 1)^\top$ in the BEV image I'. The wrapping function is given by:

$$\mathbf{p}' \propto \mathbf{G}\,\mathbf{p} \tag{2}$$

where $\mathbf{G}$ is the collineation matrix ensuring the IPM transformation from I to I'. $\mathbf{G}$ can be expressed in terms of the intrinsic matrix $\mathbf{K}$ and the Euclidean homography matrix $\mathbf{H} \in \mathbb{SL}(3)$ related to a planar viewed object. Note that $\mathbf{H}$ depends on the rotation matrix $\mathbf{R}$ and the translation vector $\mathbf{t}$ corresponding to the rigid transformation between the real camera pose providing the image I and the virtual one where I' is generated.

In the context of this work, the real camera is rigidly fixed on the P2WV main body and not affected by the steering motion. We assume that the camera pitch, roll angles and its height above the ground level are denoted respectively by μ, ϕ and h_c as depicted in Figure 2 in [13]. Let us assume that ϕ and h_c are measured since we know the

camera mounting height z_c and $h_c = z_c \cos(\phi)$. In addition, we shall assume the pitch angle constant when dealing with the estimator synthesis. It will be considered as equal to the known mounting tilt angle of the camera $\mu = \mu_0$. The relative yaw angle between the vehicle and the road trajectory can not be measured since, in our case, the road map is not available. Nevertheless, they are supposed to be very close since the rider follows the road. However, in case of over or under-steering regarding the road curvature, it results in a BEV image rotation around its virtual optical axis (Z-axis) which is perpendicular to the ground and does not impact the algorithm derived in the next section. Finally, the rotation matrix $\mathbf{R}$ is given by $\mathbf{R} = \mathbf{R_c}\mathbf{R}_\phi\mathbf{R}_\mu$ with $\mathbf{R_c}$ being the fixed rotation matrix to align the camera Z-axis with the longitudinal X-axis of the vehicle coordinate system. $\mathbf{R}_\phi$ and $\mathbf{R}_\mu$ are the rotation matrices associated to the roll and pitch angles respectively. Their expressions are given in [13].

Let $\mathcal{F}_v$ be a 3D frame attached to the P2WV whose origin is the projection of the optical center on the road plane defined by $Z = 0$ (illustration is given in [13]). $\mathcal{F}_v$ is oriented such that X is parallel to the vehicle longitudinal axis and Z points upward. In addition, let us assume that all the points belonging to the road lie on the same plane XY of $\mathcal{F}_v$. In this case, the aim of the IPM is to generate a top-view of this plane by projecting back all the points from the captured 2D image I to the plane XY of the 3D frame $\mathcal{F}_v$. Finally, the BEV is obtained by cropping the top-view of the plane according to the desired Region Of Interest (ROI). Note that this transformation is none other than the homography relationship.

Under the assumptions given above, the IPM transformation based on the collineation matrix $\mathbf{G}$ depends only on angles ϕ and μ, the camera calibration matrix $\mathbf{K}$, the camera height h_c, the desired resolution of the output image and the ROI. The latter is defined by its top-left and the bottom-right points of coordinates (X_{max}, Y_{max}) and (X_{min}, Y_{min}) in the 3D vehicle frame $\mathcal{F}_v$.

The collineation matrix $\mathbf{G}$ can be easily identified in two steps. If we use the assumptions $Z = 0$ and $\mathbf{t} = (0\ 0\ -h_c)^\top$ in equation (1), we obtain:

$$\mathbf{p} \propto \mathbf{K}\,\mathbf{M}\,\mathbf{p_w} \tag{3}$$

where $\mathbf{M} = (r_1\quad r_2\quad -h_c r_3)$ with r_i the column i of the rotation matrix $\mathbf{R}$. p_w is a point of homogeneous coordinates $\mathbf{p_w} = (X\ Y\ 1)^\top$ lying on the plane $Z = 0$ in the frame $\mathcal{F}_v$. Whereas $\mathbf{p} = (u\ v\ 1)^\top$ is its projection into the image I.

The relation between p_w and p' is obtained by cropping the top-view regarding the desired ROI and output BEV resolution. If the output resolution is $(n' \times m')$, then :

$$\mathbf{p}' = \mathbf{S}\,\mathbf{p_w} \tag{4}$$

with $\mathbf{S} = \begin{pmatrix} 0 & -m'\frac{1}{\Delta Y} & m'\frac{Y_{max}}{\Delta Y} \\ -n'\frac{1}{\Delta X} & 0 & n'\frac{X_{max}}{\Delta X} \\ 0 & 0 & 1 \end{pmatrix}$, $\Delta X = X_{max} - X_{min}$ and $\Delta Y = Y_{max} - Y_{min}$.

Finally, from the equations (2), (3) and (4) it comes:

$$\mathbf{G} = \left(\mathbf{K}\,\mathbf{M}\,\mathbf{S}^{-1}\right)^{-1} \tag{5}$$

In other words, the BEV image I' is obtained by warping each point in I' onto I using the inverse mapping $\mathbf{G}^{-1}$ and then the image intensity is computed by interpolating the local pixels intensities in the origin image I. An example of BEV image is shown in Figure 1.

B. Road Lane detection and fitting

In the race for new ADAS, the road marker detection has been widely addressed in the past years. In this work, we used the method recently proposed in [13]. It is based on the intensity gradient between the road separation lane markers and their surroundings. It allows the detection of both straight and curved separation lanes and requires few computing resources. Moreover, this method turns out to be a very appropriate solution to detect the separation lanes in a BEV image since it takes into account the line width, denoted w, as a filtering parameter. Note that the properties (width, length, etc.) are precisely defined in the road design specifications. Then the filtered image is thresholded and re-filtered to respectively keep only the lane objects in a new binary image and remove the small blobs. Once the binary image of the separation lane markers I'' is obtained, one aims to separate the lanes (left, center and right in our case). To that end, a sliding window algorithm is used to track each separation lane independently in I''.

When investigating the road design literature, it appears that the well-known clothoid model was largely adopted to design roads [14]. The clothoid-based design ensures smooth transitions between straight and curved lines helping drivers to track the road markers and avoiding abrupt changes in steering direction. It is defined such that the length of the curve l from the curve origin must be proportional to the curvature. Hence, the following expression was introduced in the literature by [14]:

$$C(l) = C_0 + C_1 l \qquad (6)$$

where C_0 and C_1 are respectively the initial curvature and its rate along the curve. Note that this model is only valid for horizontal curves when the road is planar. As in [13], if we consider the heading angle between the road tangent and the vehicle X-axis is small (less than $10°$), equation (6) can be approximated in the Cartesian coordinate system with a third order polynomial expression:

$$y(x) \approx a_0 + a_1 x + a_2 x^2 + a_3 x^3 \qquad (7)$$

with a_i the coefficients of the polynomial function. To get the expressions of the coefficients a_i as a function of the road geometry parameters and the vehicle relative position, the reader can refer to [13].

IV. ROLL ANGLE ESTIMATION

This section discusses the technique to estimate the vehicle roll angle from the camera images. Note that in this work we used the algorithm for motorcycle estimation purpose but it can be utilized for other vehicles without any restriction. Let us remind that the roll angle is one of the most crucial risk indicator when studying vehicle lateral safety. Our method

is capable of estimating the absolute roll angle to the road without any influence of the bank angle. Note that the estimation of the road bank have motivated several works as in [15] because this is a crucial parameter when estimating the tire's forces. For that purpose, our estimator can be coupled with an IMU allowing directly to get the bank angle after computing a simple difference between the measured roll and the estimated one.

In a world where the autonomous vehicle is making its own place, it is obvious the infrastructure will be improved to facilitate the guidance of this new generation of vehicle. The design of this car is highly complex and requires advanced computer vision algorithms which detect the environment and especially the road. In this context, ones of the most important markers are the separation lanes. Hence, we can imagine, in a near future, the horizontal road signalization will be improved on many roads. The algorithm presented below is thought in this context since it requires at least 3 distinct separation lanes. These road markers can be dashed or solid but they must be as parallel as possible which is the case most of the time.

To derive the estimator we will assume the camera pitch angle is known since we will consider it as equal to the mounting tilt angle. In addition, its dynamics is not taken into account. It is consistent because pitch motions mainly occur when accelerating or braking hard which never happen when the P2WV is leaned. Furthermore, according to the road design specifications, the road slope vary slowly to avoid abrupt changes. It allows one to consider that the road is planar in the ROI of the BEV. However, there is no assumption about the road bank.

The proposed roll angle estimator is based on the prior knowledge of the road separation lane geometric properties in the BEV. Indeed, in a perfect top-view of the road we know that the markers delimiting the road are supposed to be parallel. In addition, the road track widths are supposed to be equal meaning the markers are equidistant. According to this finding, the algorithm performs a numerical loop increasing the roll angle of $\delta\phi$ at each iteration until the lanes appear as parallel and equidistant in the BEV. The process is illustrated in Figure 1.

For a captured image I_i, the algorithm generates a first BEV with the IPM technique using the previous estimated value of the roll angle denoted $\hat{\phi}_{i-1}$. We use the previous roll estimation to initialize the estimator in order to save computation time. Note that, even if we consider the previous estimation in the current loop, the estimated roll is not relative to the previous sample. Because of the incorrect roll angle, the obtained BEV image is deformed and does not correspond to the ideal top-view. Then, the algorithm looks for the solution in a predefined roll range denoted $\Delta\phi$. This method does not require any knowledge of the sign of the roll motion. In the case where the previous roll is not taken into account $\Delta\phi$ must include all the feasible roll angles. Usually, it leads to $\Delta\phi = [-50°, 50°]$. However, to accelerate the algorithm the range can be reduced with regards to the camera recording speed and centered around
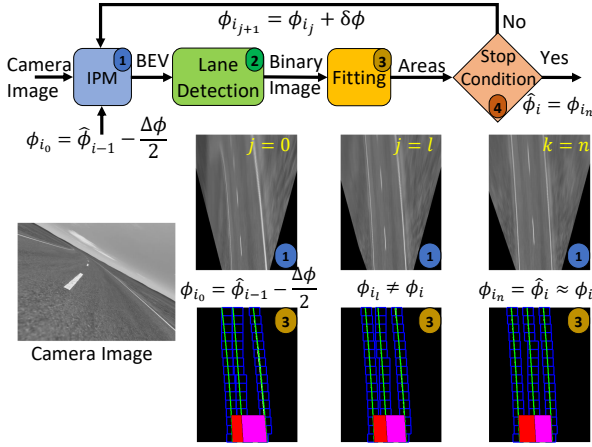
Fig. 1: Roll angle estimation method

the previous estimated roll angle $\hat{\phi}_{i-1}$. According to our best knowledge, in severe riding situations where the roll dynamics is highly excited, the roll rate rarely exceed $|\dot{\phi}| < 60°.s^{-1}$. If we consider a basic camera recording at 30 fps, it means, in extreme scenarios, the roll can not change more than 2 degrees between two consecutive images. It leads to $\Delta\phi = [-2° + s_{\Delta\phi}, 2° + s_{\Delta\phi}]$ with $s_{\Delta\phi}$ a safety coefficient which makes the range a bit larger to take into account the roll estimation uncertainties.

Although the estimator algorithm is intuitive, the stop condition needs to be wisely chosen. Instead of comparing the coefficients a_i of each lane given in (7) until detecting equidistant and parallel lanes, the stop condition is defined as an area comparison. After obtaining the third order polynomial functions for the 3 separation lanes, we can compute the areas between the center-left and the center-right lanes like in Figure 1. Note that we have selected a ratio of the BEV image to reduce the uncertainties due to the dashed center lane approximations. This area stop condition is more robust against the pitch errors. Indeed, even if the pitch motion is neglected, in real situation small motions happen. For an iteration j, if the difference of these two areas (represented in red and magenta in Figure 1) is inferior to a given threshold, then we stop the iteration loop $\hat{\phi}_i = \phi_{i_j}$. With ϕ_{i_j} denoting the roll angle for the image i at the loop iteration j. Otherwise, the algorithm performs another loop with the new value of the roll angle given by $\phi_{i_{j+1}} = \phi_{i_j} + \delta\phi$.

Another illustration of the problem is to consider that the IPM generates a virtual camera whose optical axis is not exactly perpendicular to the road plane. The aims of the algorithm is to rotate this virtual camera until we see the road separation lanes appearing as parallel and equidistant meaning the virtual camera axis is perpendicular to the road.

Finally, for a captured image I_i the algorithm can be summarized by the following steps:

1) Compute the BEV with ϕ_{i_j} as roll angle. For the first iteration, $\phi_{i_0} = \hat{\phi}_{i-1} - \Delta\phi/2$.

2) Filter and track the 3 road separation lanes.
3) Fit the road markers with third order polynomial functions and compute the right and left areas.
4) Compute the difference between the two areas. Is the result inferior to the threshold? Yes, $\hat{\phi}_i = \phi_{i_j}$ and exit the loop. No, $\phi_{i_{j+1}} = \phi_{i_j} + \delta\phi$ and go back to step 1 with updating ϕ_{i_j}.

Note that the performances of the algorithm are highly dependent of the settings. It depends directly on the size of the roll range $\Delta\phi$ and the roll loop resolution $\delta\phi$. The larger the roll range is, the longer the computation time is. This observation is also true for small roll resolution $\delta\phi$. Moreover, a smaller $\delta\phi$ leads to a more accurate estimation. It requires finding a compromise depending of the algorithm application.

V. BIKESIM SIMULATION RESULTS

This section validates the proposed algorithm on various scenarios using the advanced motorcycle simulator BikeSim.

The camera was virtually installed in front of the P2WV at a height $z_c = 1.10$ m and mechanically tilted by an angle $\mu_0 = 12°$. The ROI is chosen large enough to capture the left, center and right lanes with $Y_{max} = -Y_{min} = 15$ m. In addition, $X_{max} = 20$ m and $X_{min} = 5$ m to respectively capture more than one piece of the center dashed lane and to avoid blind spot consideration. The camera recording speed is set at 30 fps whereas, its resolution to (640x480) and its pixelic focal lengths are adjusted such that $f_u = f_v = 380$ pixels. Note that this kind of camera is largely widespread. Nevertheless, in the section discussing the results we will compare the results with a higher camera resolution at (1080x720). To facilitate the filtering and fitting steps, we will assume that the BEV image I' is of size $(m \times n)$ since the original image I is of size $(n \times m)$.

The proposed algorithm was tested under several different scenarios and two of them are presented below. In these two scenarios, we assume the two-lane road to be planar and the three separation lanes (right, center and left) are structured and detectable.

A. Scenic road

A constant speed scenic road simulation at 100 km/h is presented first. This scenario simulates an extra-urban road which is composed of straight lines, circular turns and clothoids to ensure smooth connections (see Figure 2). This kind of scenario is particularly interesting in the development of ARAS since it is one of the most deadly. This is because of the high ratio between road curvature and speed limits. Indeed, urban roads can have more aggressive turns but the speed limit is slower although on a highway the speed limit is faster but the curve radius are very large. In addition, with its large roll angles as illustrated in Figure 2, this simulation tests the algorithm during an aggressive riding scenario.

Figure 2.a and 2.b depicts the vehicle trajectory along the scenic road scenario and the corresponding motorcycle roll, yaw and pitch angles. We can observe the pitch angle, in orange, is almost constant as discussed in the assumptions.

Whereas Figures 2.c presents the estimated roll angle, in red, and the actual ones, in blue. One can remark some estimation errors especially for the large roll angles. This could be explained by the lane detection uncertainties, the road clothoid model approximation combined with the numeric resolution $\delta\phi$.
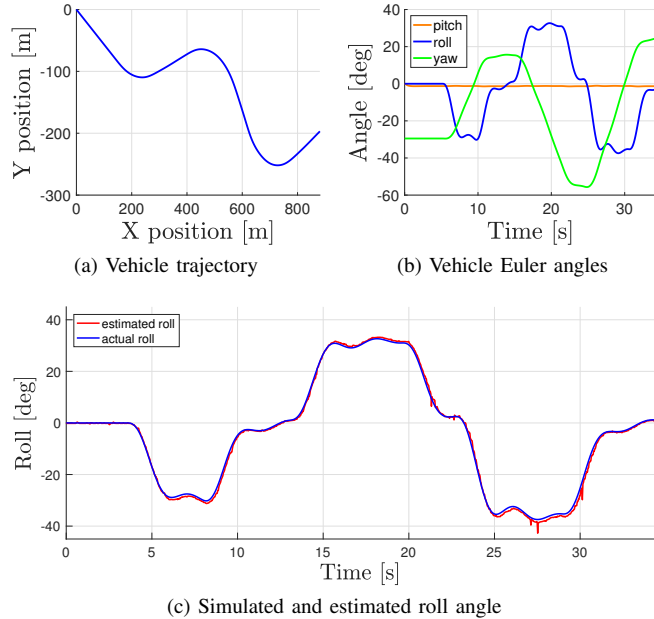

(a) Vehicle trajectory

(b) Vehicle Euler angles

(c) Simulated and estimated roll angle

Fig. 2: Scenic road scenario at 100 km/h

Moreover, this finding confirms that the estimation uncertainties depend on the roll angle. In practice, when the camera is significantly leaned, some captured objects are represented with more or less pixels in the image (see the captured image in Figure 1). It depends where these objects are located with respect to the camera position. Note that the estimation performances are discussed in detail in the next section but this first figure gives a first idea about the observer capabilities.

B. Double lane change

The Double Lane Change (DLC) is a well-known scenario in the development of ADAS since it is an obstacle avoidance maneuver. In addition to test the proposed algorithm on an emergency riding scenario, the DLC allows to test a very specific case too. Indeed, the road is straight whereas the vehicle has a large lateral deviation which is a rare case where the vehicle trajectory significantly differs from the road route. Like for the scenic road the riding speed is assumed constant at 100 km/h.

Figure 3.a depicts the P2WV trajectory during the DLC, the vehicle is initially in a straight trajectory and suddenly crosses the center lane to avoid an obstacle before going back to its initial lateral position. Whereas Figure 3.b shows that even if the road shape is straight, a DLC maneuver with a P2WV highly excites the lateral dynamics. As for the scenic road, Figures 3.c presents the roll estimation results. One can observe again estimation errors which are more visible

because of the time scale and the specific DLC trajectory. Indeed, the road clothoid model given in (7) is valid for small heading angle.
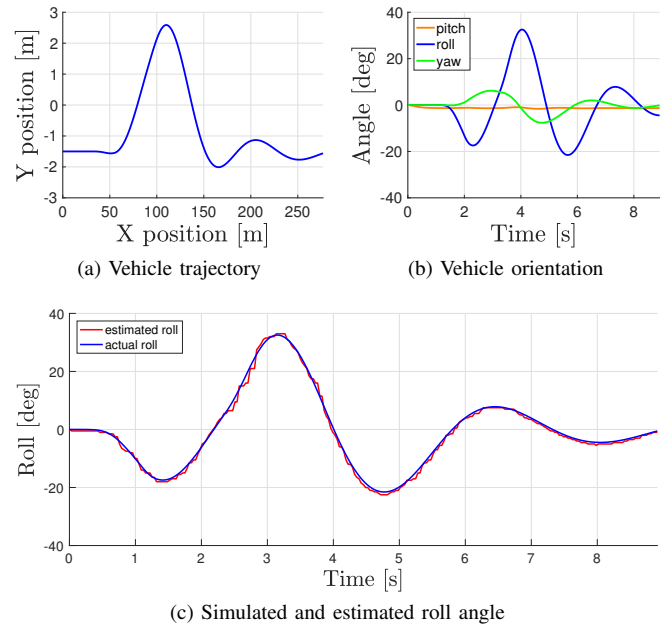

(a) Vehicle trajectory

(b) Vehicle orientation

(c) Simulated and estimated roll angle

Fig. 3: Double lane change scenario at 100 km/h

Whereas, the DLC scenario involves significant vehicle heading deviation with respect to the straight road trajectory (see Figure 3). As previously, the lane detection and the road model uncertainties combined with the numeric resolution contribute to these errors. Nevertheless, even if the DLC is near the limit of the clothoid model, the estimation performances are largely acceptable.

C. Result discussion

This subsection discussed the above results and presents a Root-Mean-Square Error (RMSE) study which is a well-known technique to contrast the estimation errors. For more information about the RMSE expression please refer to [13]. For both simulations, the roll resolution and the range are set such that $\delta\phi = 0.5°$ and $\Delta\phi = 6°$. Figures 2.c and 3.c demonstrates all the potential of the proposed method. The results can be compared to what a low cost IMU could measure. Nevertheless, we can see a slight estimation error when the roll angle is large due to lane detection approximations. Even with this slight error our method is more effective than most of the model-based estimators proposed in the literature. Indeed, these last are often designed for a nominal case with linear assumptions and because of uncertainties the estimation can be degraded [9].

In Table I, the RMSE is computed for both camera resolutions ((640x480) and (1080x720)) for the DLC scenario. Moreover, the parameter τ denotes the computation time performance as the ratio between the total estimation time and the simulation time at a recording speed of 30 fps. The simulation was carried out on macOS with a 3.1 GHz Intel

Core i7 CPU. Of course deploying the algorithm on a real-time OS with optimized image processing toolboxes could give much better performances but this first study gives a first idea about the algorithm speed.

		Camera Resolution	
		(640x480)	(1080x720)
$\delta\phi = 0.1°$	RMSE [ ]	$1.77e^{-1}$	$0.91e^{-1}$
	τ [%]	621.1	934.5
$\delta\phi = 0.5°$	RMSE [ ]	$7.97e^{-1}$	$5.81e^{-1}$
	τ [%]	334.8	503.4
$\delta\phi = 1°$	RMSE [ ]	$8.25e^{-1}$	$6.99e^{-1}$
	τ [%]	182.1	310.5

TABLE I: RMSE RESULTS FOR THE DLC

This table endorses some intuitive observations. If we increase the camera resolution the estimation performances are undoubtedly better. It comes from the noise reduction during the filtering and approximating step of the road lanes. Moreover, as expected the estimation accuracy directly depends on the numeric resolution of the roll loop. Nevertheless, the time performance analysis demonstrates that increase the resolution or decrease the numeric resolution have serious consequences on the computation time making this algorithm far from being a real time solution.

Although this solution show a strong capability of estimating the roll without any vehicle or tire model the algorithm needs to be improved to be real time. Indeed, even for a low image resolution at (640x480) and a large roll step $\delta\phi = 1°$ it takes about 1.8 times more than the time required to simulate the scenario. Nevertheless, in term of time performances, the algorithm could be optimized by defining the roll resolution $\delta\phi$ as a function of the areas difference. It means, if the difference is important $\delta\phi$ is increased, whereas if it is small, we know we are near the solution, we reduce $\delta\phi$.

VI. CONCLUSION

This paper introduced a vision-based algorithm to estimate the absolute P2WV roll angle to the road using only a basic monocular camera. Note that it is illustrated on motorcycle estimation but there is no restriction to generalize the solution for other kind of vehicle. The roll angle is one of the most important risk indicator for lateral P2WV safety purposes. Its estimation has been largely addressed in the literature with model-based approaches and heavy instrumentation. Nevertheless, these solutions work well under restrictive assumptions around nominal cases. The method discussed in this paper, only depends on the camera parameters and is insensitive to other parameters such that the rider weight.

The algorithm is based on prior knowledge of the road markers. For each captured image, the algorithm creates a virtual camera which is rotated until the road markers appear parallel and equidistant in the virtual image. It performs an IPM transformation using the previous estimated roll.

Finally, we get an approximate BEV where the road lanes are filtered and tracked. Then, a fitting step allows to approximate the lanes with third order polynomial functions and to compute two distinct areas between the left-center and right-center lanes. Then, this two areas are compared to detect if the lanes are parallel and equidistant. If the image does not conform to the requirements the roll angle defining the position of the virtual camera is increased by the roll resolution $\delta\phi$. The loop is repeated until the area difference is inferior to a defined threshold. The solution was tested on various test scenarios including a scenic road and a DLC with two camera resolutions. Furthermore, a RMSE study on DLC scenario was discussed in order to compare the performances in terms of accuracy and computing time for two camera resolutions.

The results discussed in this paper are very promising and open a real alternative to model-based approaches to estimating the P2WV roll angle. The next step will deal with algorithm optimization to perform real time estimation and validate the approach on experimental data.

REFERENCES

[1] E. Fussl and al, "Riders acceptance of advanced rider assistance systems," *ITS World Congress*, 2012.
[2] I. Boniolo, M. Norgia, M. Tanelli, C. Svelto, and S. M. Savaresi, "Performance analysis of an optical distance sensor for roll angle estimation in sport motorcycles," *IFAC World Congress*, 2008.
[3] I. Boniolo, S. M. Savaresi, and M. Tanelli, "Roll angle estimation in two-wheeled vehicles," *IET Control Theory Applications*, 2009.
[4] I. Boniolo and S. M. Savaresi, "Motorcycle lean angle estimation with frequency separation principle and angular rates measurements," *IFAC World Congress*, 2010.
[5] A. Teerhuis and S. Jansen, "Motorcycle state estimation for lateral dynamics," *Vehicle System Dynamics (VSD)*, 2012.
[6] P.-M. Damon, M. E.-H. Dabladji, D. Ichalal, L. Nehaoua, and H. Arioui, "Estimation of lateral motorcycle dynamics and rider action with luenberger observer," *Conference on Intelligent Transportation Systems (ITSC)*, pp. 2392–2397, Nov 2016.
[7] P. M. Damon, M. E.-H. Dabladji, D. Ichalal, L. Nehaoua, H. Arioui, and S. Mammar, "Lateral motorcycle dynamics and rider action estimation: An LPV unknown input observer approach," in *Conference on Control Applications (CCA)*, Sept 2016, pp. 711–716.
[8] P.-M. Damon, D. Ichalal, H. Arioui, and S. Mammar, "Cascaded flatness-based observation approach for lateral motorcycle dynamics estimation," *Conference on Systems, Man, and Cybernetics (SMC)*, pp. 3243–3248, 2017.
[9] P.-M. Damon, D. Ichalal, L. Nehaoua, and H. Arioui, "Lateral & steering dynamics estimation for single track vehicle: Experimental tests," *IFAC World Congress*, vol. 50, no. 1, pp. 3400 – 3405, 2017.
[10] M. Schlipsing, J. Schepanek, and J. Salmen, "Video-based roll angle estimation for two-wheeled vehicles," *Intelligent Vehicles Symposium*, pp. 876–881, June 2011.
[11] M. Schlipsing, J. Salmen, B. Lattke, K. G. Schröter, and H. Winner, "Roll angle estimation for motorcycles: Comparing video and inertial sensor approaches," *Intelligent Vehicles Symposium*, 2012.
[12] M. Barnada, C. Conrad, H. Bradler, M. Ochs, and R. Mester, "Estimation of automotive pitch, yaw, and roll using enhanced phase correlation on multiple far-field windows," *Intelligent Vehicles Symposium*, 2015.
[13] P.-M. Damon, H. Hadj-Abdelkader, H. Arioui, and K. Youcef-Toumi, "Image-based lateral position, steering behavior estimation, and road curvature prediction for motorcycles," *Robotics and Automation Letters (RAL)*, vol. 3, no. 3, pp. 2694–2701, July 2018.
[14] E. D. Dickmanns and A. Zapp, "A curvature-based scheme for improving road vehicle guidance by computer vision," *Proc.SPIE*, 1987.
[15] J. Ryu and J. C. Gerdes, "Estimation of vehicle roll and road bank angle," *American Control Conference (ACC)*, 2004.